Less reliable water availability in the 21st century climate projections

Sanjiv Kumar, David M. Lawrence, Paul A. Dirmeyer & Justin Sheffield

2014

AGU PUBLICATIONS

Earth's Future

COMMENTARY

10.1002/2013EF000159

Key Points:
- Decreased water availability in dry season
- Increased water availability in wet season
- Increased floods and droughts in future climate

Supporting Information:
- Supplementary_material_rev1.pdf
- Readme_rev1.docx

Corresponding author:
S. Kumar, sanjiv@cola.iges.org

Citation:
Kumar, S., D. M. Lawrence, P. A. Dirmeyer, and J. Sheffield (2013), Less reliable water availability in the 21st century climate projections, *Earth's Future*, *2*, 152–160, doi:10.1002/2013EF000159.

Received 21 AUG 2013
Accepted 10 DEC 2013
Accepted article online 17 DEC 2013
Published online 10 MAR 2014

Less reliable water availability in the 21st century climate projections

Sanjiv Kumar[1,2], David M. Lawrence[2], Paul A. Dirmeyer[1], and Justin Sheffield[3]

[1]Center for Ocean-Land-Atmosphere Studies, George Mason University, Fairfax, Virginia, USA, [2]National Center for Atmospheric Research, Boulder, Colorado, USA, [3]Department of Civil and Environmental Engineering, Princeton University, Princeton, New Jersey, USA

Abstract The temporal variability of river and soil water affects society at time scales ranging from hourly to decadal. The available water (AW), i.e., precipitation minus evapotranspiration, represents the total water available for runoff, soil water storage change, and ground water recharge. The reliability of AW is defined as the annual range of AW between local wet and dry seasons. A smaller annual range represents greater reliability and a larger range denotes less reliability. Here we assess the reliability of AW in the 21st century climate projections by 20 climate models from phase 5 of the Coupled Model Intercomparison Project (CMIP5). The multimodel consensus suggests less reliable AW in the 21st century than in the 20th century with generally decreasing AW in local dry seasons and increasing AW in local wet seasons. In addition to the canonical perspective from climate models that *wet regions will get wetter*, this study suggests greater dryness during dry seasons even in regions where the mean climate becomes wetter. Lower emission scenarios show significant advantages in terms of minimizing impacts on AW but do not eliminate these impacts altogether.

Summary Modeling of future water availability predicts that wet regions become wetter and dry regions become drier, leading to an increasing likelihood of seasonal droughts and floods in regions where such vulnerability is already high.

1. Introduction

The temporal variability of river and soil water affects society at time scales ranging from hourly to decadal. A few hours of intense rain, for example, can result in flooding, and seasonal precipitation deficits manifest into droughts, which may persist for years. Humans attempt to even out the temporal variability of precipitation through massive interventions in the hydrological system, primarily through the construction of dams and reservoirs and the utilization of irrigation to maintain high crop productivity in dry situations. One of the important questions with respect to projected future climate change is whether existing or planned human interventions in the water cycle will be able to adequately meet future demands as both climate and water demands change. Here we utilize data from phase 5 of the Coupled Model Intercomparison Project (CMIP5) [*Taylor et al*., 2012] simulations to assess projected changes in the availability of water throughout the year, with particular focus on wet and dry season water availability.

Many studies have shown that significant changes in mean annual runoff could occur under various climate change scenarios [e.g., *Milly et al*., 2005; *Tang and Lettenmaier*, 2012; *Arnell and Gosling*, 2013]. Typical projected changes in annual runoff include increases at high latitudes and in the moist tropics and decreases over midlatitude western North America, Central Europe, the Mediterranean region, and most dry subtropical regions. While the role of precipitation change in runoff trends is well recognized [*Kumar et al*., 2009], the role of evapotranspiration has been investigated to a lesser extent [e.g., *Okazaki et al*., 2012]. The relative contribution of evapotranspiration to the water budget becomes increasingly important in climate projections because the precipitation response to global warming is much weaker (~2%/K) than the Clausius-Clapeyron relationship that controls humidity (7%/K) [*Held and Soden*, 2006]. Consequently, evapotranspiration from the land surface becomes progressively more water-limited [*Kumar et al*., 2013]. Here we use a new metric for seasonal water availability that incorporates both the precipitation and the evapotranspiration responses under climate change.

A canonical perspective of the impact of climate change on the water cycle is that wet regions will get wetter and dry regions will get drier [*Held and Soden*, 2006; *Chou et al*., 2009]. *Chou and Lan* [2012] suggest

that locally also there may be increasing trends in the annual precipitation range, i.e., at a given location the wet season becomes wetter and the dry season becomes drier. There is already some indication in the historical record that this expansion of the annual precipitation range is happening, though uncertainties are considerable [*Chou et al*., 2013]. These precipitation changes combined with evapotranspiration changes are likely to alter the reliability of water availability. The reliability of available water (AW) is defined as the annual range of AW between local wet and dry seasons. A smaller annual range represents greater reliability and a larger range denotes less reliability. Here we have conducted a comprehensive assessment of CMIP5 climate models regarding projected changes in AW reliability.

2. Data and Method

Twenty CMIP5 climate models are included in this analysis. We have employed "historical" simulations for the 20th century climate and several representative concentration pathway (RCP) simulations for the 21st century climate. RCPs represent projected future socioeconomic conditions, technological development, and society's climate choices [*Moss et al*., 2010]. RCP8.5 represents a "no climate policy" world with high population growth, slow economic development, and modest technological advances, leading to the highest CO_2 equivalent concentration by 2100 representing a 8.5 W m^{-2} net radiative impact on the Earth's surface (~1370 ppm) [*Riahi et al*., 2011]. At the other end of the scenario spectrum, RCP2.6 represents 2.6 W m^{-2} net radiative impact with a stringent mitigation scenario that reduces CO_2 emissions by using bioenergy, technological advances, and socioeconomic development (higher income and slower population growth) and reaches a peak CO_2 equivalent concentration of 490 ppm before 2100. RCP4.5 (4.5 W m^{-2}) is a mixed scenario that stabilizes CO_2 emissions to 650 ppm CO_2 equivalent concentration by 2100 [*van Vuuren et al*., 2011]. Developers of RCP scenarios do not assign any preference to one RCP compared with others [*van Vuuren et al*., 2011]. However, considering little has been done to stabilize greenhouse gas emissions over the last 20 years [*Tollefson and Gilbert*, 2012] and there is no realistic plan to do so in the near future [*Nature Editorial*, 2012], we have given preference to the RCP8.5 scenario. We have also presented comparisons with RCP4.5 and RCP2.6 scenarios to determine how much benefit can be accrued by making climate choices that reduce or stabilize greenhouse gas emissions.

Only one ensemble member from each model/experiment (mostly the first member, but if not available then second ensemble member) is used. Prior to analysis all models are regridded to a common resolution of 2.5° × 2.5° (144 × 72 global grid) using an area-average preserving method (area_conserve_remap_wrap function in The NCAR Command Language) [*UCAR/NCAR/CISL/VETS*, 2013].

Monthly AW is defined in equation 1.

$$AW_{m,y} = \frac{P_{m,y} - ET_{m,y}}{\left(\overline{P}\right)_{\text{present}}}, \tag{1}$$

where $AW_{m,y}$ is available water for a given month (m) and year (y), $P_{m,y}$ and $ET_{m,y}$ are precipitation and evapotranspiration for the given month and year, and $\left(\overline{P}\right)_{\text{present}}$ is the present annual climatological mean (calculated for 1961–1990, same value for all 12 months) precipitation at a given location (grid cell) and a given model. The denominator $\left(\overline{P}\right)_{\text{present}}$ is a spatial normalization factor to account for spatial variability in total precipitation. We have kept the denominator the same for present and future climate, thereby quantifying absolute changes in (P − ET) from present to future climate. AW is the total water available for runoff, soil water storage change, and ground water recharge [*Schuol et al*., 2008]. A negative AW represents stress on surface water storages from atmospheric demand. We calculated 12 three-month seasonal means (December-January-February (DJF), January-February-March (JFM), and so on) for each year, and identified the maximum and minimum value within these 12 "seasons" as the wet and dry season AW in a given year. We also calculated the percentage benefit from the RCP4.5 and RCP2.6 scenarios relative to the RCP8.5 scenario as:

$$\%\text{benefit} = \left(1.0 - \frac{AW_{RCPx} - AW_{Historical}}{AW_{RCP8.5} - AW_{Historical}}\right) * 100, \tag{2}$$

where RCPx is RCP2.6 or RCP4.5. Formulae for other statistical measures used in this study are given in the supporting information.

To account for the effect of natural variability (decadal to multidecadal) in the present climate, we calculated 30 random 30-year climatologies ending anywhere between 1975 and 2004, e.g. (1945–1975), (1963–1992), (1952–1981), … (1975–2004), and then calculated the standard deviation across these 30 random climatologies in the respective seasons. A change is significant at the 95% confidence interval if its magnitude is greater than 2 climatological standard deviations in a given model, and 65% or greater models have same sign of change. This methodology ensures consistency in a given model. However, because much of the 30-year climatology is overlapping, we used 2 standard deviation measures instead of 1 standard deviation used by *Arnell and Gosling* [2013] by employing nonoverlapping periods. Estimation of natural variability is only indicative. Long control climate simulations are needed to robustly estimate the effects of natural variability.

The AW index differs from previously utilized water indices [e.g., the Supply Demand Drought Index, SDDI, *Rind et al*., 1990 and the Palmer Drought Severity Index, PDSI, *Palmer*, 1965] in several important respects: (1) the AW index is based on "actual" (climate model) ET rather than potential ET (PET), which is used in the SDDI and PDSI. (2) By design, the SDDI and PDSI exhibit significant autocorrelation from month to month, hence they are suitable primarily for the study of drought. On the other hand, floods are relatively short-term events, and we show later that the AW index is well suited to study both short-term floods and droughts. (3) The AW index allows us to assess the annual range between wet and dry season AW because the denominator remains constant for all seasons or months at a given location, whereas in the PDSI and SDDI the denominator varies across different seasons or months. Furthermore, PET-based drought indices have important limitations: (1) they are often highly sensitive to temperature increases in future climate change scenarios [*Sheffield et al*., 2012] and (2) increased water-use efficiency by plants owing to elevated CO_2 concentration is not considered (carbon cycle feedback) [*Keenan et al*., 2013]. In global climate models, ET is constrained by water and energy balance closures [*Kumar and Merwade*, 2011] as opposed to only water balance closure in hydrology models or PDSI calculations, and many climate models include carbon cycle/vegetation feedbacks [e.g., CCSM4, *Cao et al*., 2010]. The AW is a simple index that has several advantages: (1) it can be easily calculated using climate model outputs; (2) it does not directly suffer from uncertainties in runoff parameterization; (3) it is easily interpretable in terms of long-term annual mean precipitation at a given location; and (4) it does not require empirically based water balance calculations.

3. Results

Figures 1a and 1b show interannual correlations between the driest and wettest month AW and the corresponding month Standardized Precipitation Index [SPI, *Mckee et al*., 1993] from observations and CMIP5 models. We obtained the observationally based estimates by employing two well-constrained land surface model outputs driven by observed atmospheric forcings: Global Land Data Assimilation System [GLDAS2, *Rodell et al*., 2004] and the Variable Infiltration Capacity (VIC) model [*Sheffield and Wood*, 2007]. The SPI is the most commonly used indicator of flood and droughts because of data requirements, i.e., only precipitation data, compatibility across different regional climates, and flexible time scales [*Seller et al*., 2002; *Stricevic et al*., 2011; *Du et al*., 2013]. A positive SPI indicates wet conditions and a negative SPI indicates dry conditions. In the locally driest month, we found significant positive correlation between AW and one-month SPI for 77% of the land area in the observations (average correlation coefficient: 0.52) and 66% of the land area in CMIP5 (average correlation coefficient: 0.50). Dry regions such as the southwestern United States do not show significant correlation in either observations or CMIP5. Over India, observations show significant correlation but CMIP5 does not. Studies have found limitations to SPI in dry climates, particularly in dry seasons where the precipitation distribution is highly skewed [*Mishra and Singh*, 2010]. It should also be noted that uncertainties exist in observational estimates [*Haddeland et al*., 2011]. All land areas show significant positive correlation between the wettest month AW and the corresponding month SPI (average correlation coefficient: 0.74 for observation and 0.72 for CMIP5).

Figure 1c shows the observational estimate of dry and wet season AW climatology over the midwestern United States [35°N–50°N, 80°W–98°W; *Kumar et al*., 2010]. In the 30-year climatology (1979–2008, this period is selected because of GLDAS2 data availability [satellite period]) the 1988 drought has the minimum dry season AW and the 1993 flood has the maximum AW for a wet season. Overall, the results presented in Figure 1 confirm that a decrease in the dry season AW is an indicator of more droughts and an increase in the wet season AW is an indicator of more floods.

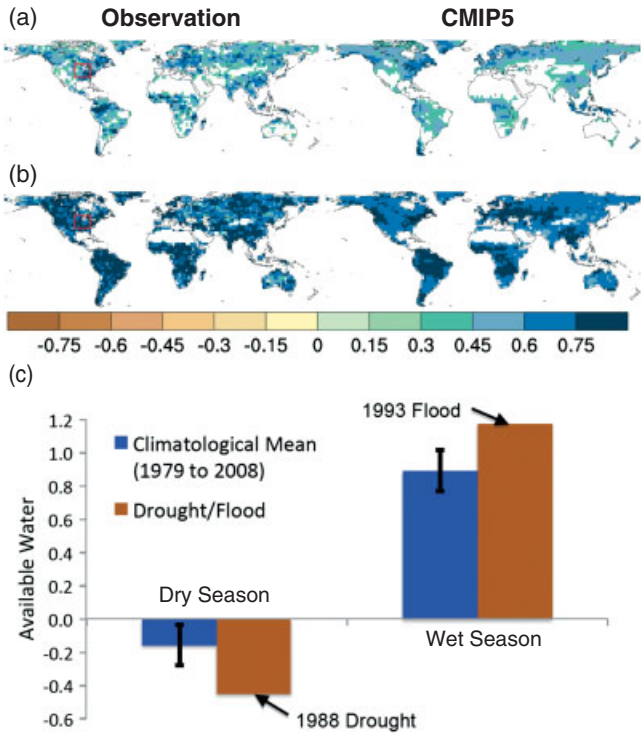

Figure 1. (a) Interannual correlation between driest month AW and the corresponding one-month SPI; (b) interannual correlation between wettest month AW and the corresponding one-month SPI; and (c) observational estimates of dry and wet season AW climatology in the midwestern United States (red box); a flood (1993) and a drought (1988) year AW are also shown. For panels (a) and (b) observational correlation is an average of GLDAS2 and VIC correlations (1979–2008) and CMIP5 is an average of 20 CMIP5 models (1975–2004). Correlations are shown only where statistically significant (>0.35 or <−0.35) in at least one of two observational estimates (GLDAS2 or VIC), and at least 10 CMIP5 models. Regions of low precipitation (<100 mm/yr) have been masked out. In panel (c), error bars represent 1 standard deviation interannual variability.

Figure 2 shows the multimodel mean monthly climatology for AW in the present (1961–1990) and future climate (2070–2099, RCP2.6 and RCP8.5). On the global scale (Figure 2a), there is a general tendency toward lower AW in drier months (e.g., MJJ) and higher AW in wetter months (NDJ). Global mean AW changes hide important regional details and magnitudes of impacts. Regionally, the changes in AW are large (Figures 2b–2d; regions are outlined in Figure 3). We first present results of the future climate in RCP8.5 scenario. RCP4.5 and RCP2.6 results are discussed later. The climatological mean dry season (JJA) AW in the North America region decreases from -0.22 ± 0.07 in the present climate to -0.36 ± 0.08 in the future climate. We represent the uncertainty range as the estimated intermodel standard error of 2.0 calculated among the 20 CMIP5 models. For Russia the dry season (MJJ) AW decreases from -0.21 ± 0.04 to -0.36 ± 0.05, and for India the dry season (JFM) AW decreases from -0.29 ± 0.06 to -0.37 ± 0.07. Consequently, the cumulative frequency (CF) of seasonally very dry conditions below a given threshold increases in the 21st century climate (Figures 2e–2g and Table 1). We calculated the CF ranging from −2.0 to 2.0 at 0.02 intervals below given thresholds considering each grid cell and each year as a single data point within the region (see the supporting information for the formula). For example, in Russia, the CF of AW ≤ -1.0 increases from $4.7 \pm 1.7\%$ in the present climate (one in every 21 years) to $12.3 \pm 2.8\%$ in the 21st century climate (one in every 8 years).

Wet season AW, on the other hand, tends to increase in the projected climate. The wet seasons for northern North America, Russia, and India are NDJ, OND, and JAS, respectively (Figures 2b–2d). In those respective seasons, the AW increases from 0.57 ± 0.04 to 0.66 ± 0.04 in northern North America, 0.80 ± 0.04 to 1.03 ± 0.04 in Russia, and 1.15 ± 0.24 to 1.59 ± 0.24 in India. Values of AW greater than 1.0 are indicative of a rainfall pattern that is highly seasonal; for example, India receives 80% of annual precipitation during the monsoon season (June to September). Consequently, the CF of very wet conditions above a given threshold increases in the 21st century climate (Figures 2h–2j). We calculated the CF ranging from −1.0 to 3.0 at 0.02 intervals above a given threshold considering each grid cell and each year as a single data point in the given region (see the supporting information for the formula). For example, in India, the CF of AW ≥ 3.0 increases from $4.0 \pm 1.0\%$ in the present climate (one in every 25 years) to $14.2 \pm 4.8\%$ in the 21st century climate (one in every 7 years).

Figures 3a and 3b show the geographical distribution of AW changes in the local dry and wet seasons (see Figure S1 in the supporting information). Much of the land area, including northern North America, Central Europe, Russia, parts of China, and India, and east-central Africa, show significant decreases in dry season AW. Some regions, such as the southwestern United States and northern Mexico, parts of Africa,

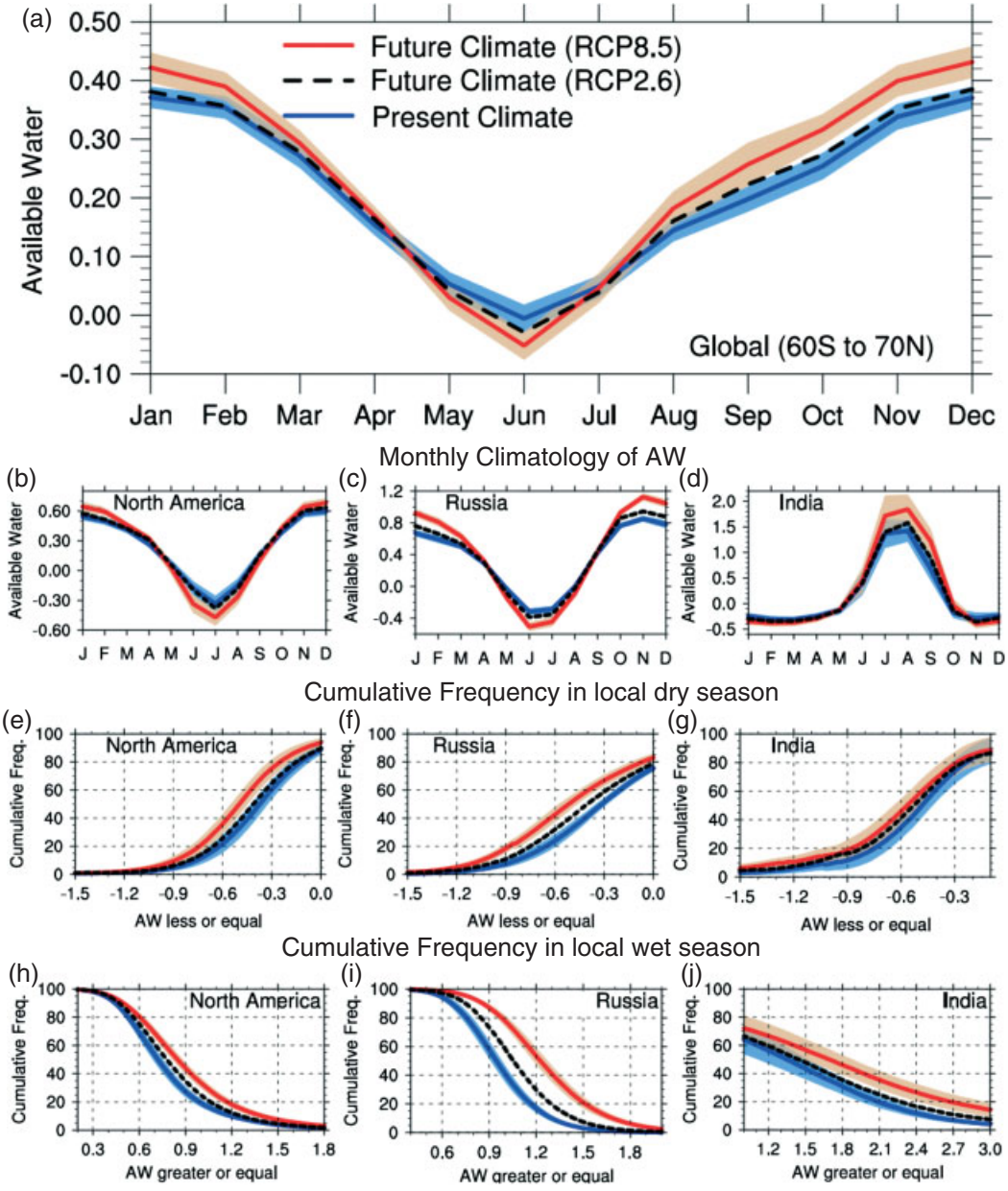

Figure 2. AW climatology and cumulative frequency in the present (1961–1990) and in the 21st century climate (2070–2099; RCP8.5 and RCP2.6). Multimodel mean and 2 standard error estimates (shading) from 20 CMIP5 climate models are shown. For clarity, only multimodel means from RCP2.6 are shown. Regions of North America, Russia, and India are outlined in Figure 3.

and South America, Alaska, and Greenland, show increases in dry season AW. However, the increases in the dry season AW in many parts of Africa and South America are not significant. Overall, 46% of the global land area exhibits a significant decrease in dry season AW, whereas only 15% shows significant increases in dry season AW.

A similar amplification of extremes is seen for AW in the wet season. Sixty percent of the global land area shows significant increases in wet season AW and 10% shows significant decreases including Mexico, southwestern Africa, the Mediterranean region, and parts of South America. The Amazon and Australia do not show significant changes in wet season AW.

Figure 4 shows the intermodel spread in global land average AW in the local wet and dry seasons including all areas of positive and negative AW changes in each respective season. There is large intermodel

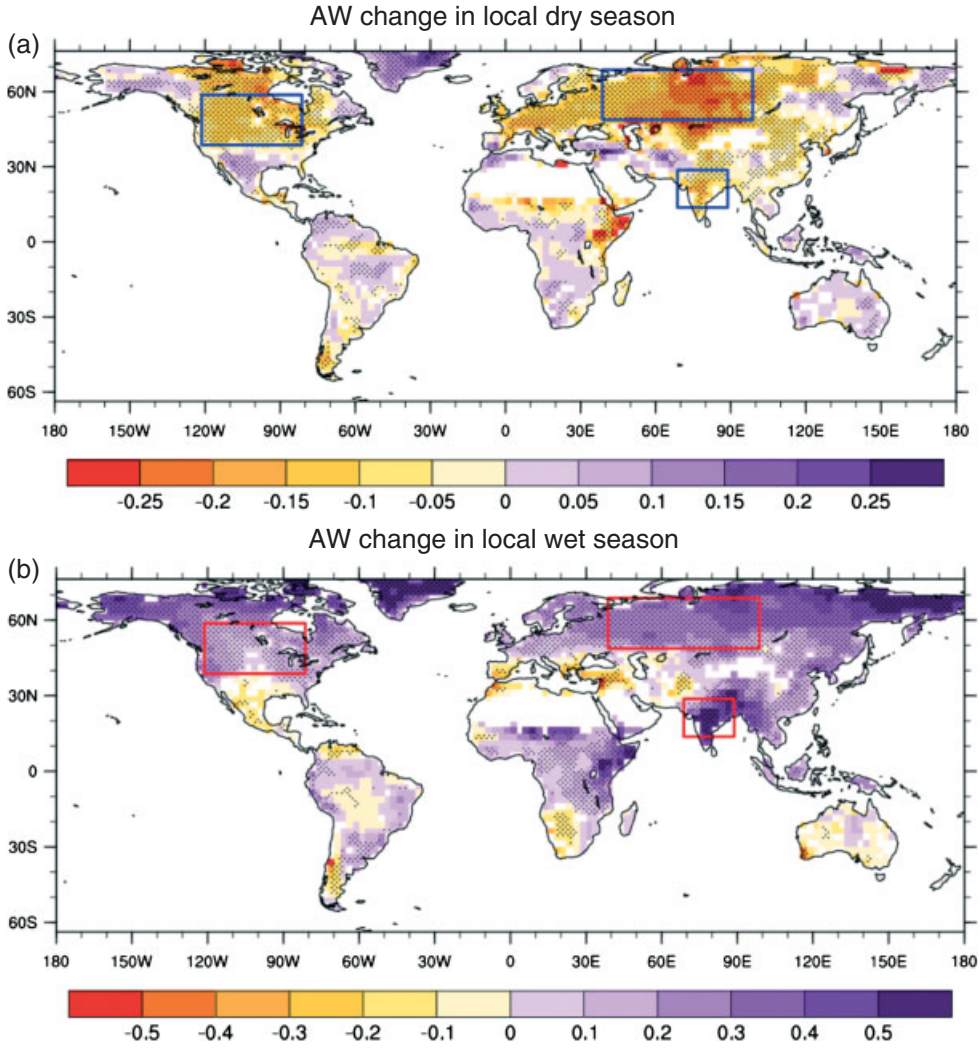

Figure 3. Changes in available water in the local dry and wet season in RCP8.5 projections (2070–2099) compared with historical simulations (1961–1990). Color shading represents at least 65% models (13 or more models out of 20) showing changes greater than 2 climatological standard deviations in the historical period. Stippling represents that at least 65% of models have the same sign of change as shown in the figure. Regions of low precipitation (<100 mm/yr) have been masked out.

spread in AW for both dry and wet season AW. For example, in the historical climate dry season AW ranges from −0.57 to −0.28 (mean: −0.38) and wet season AW ranges from 0.74 to 1.08 (mean: 0.94). In the RCP8.5 scenario, dry season AW ranges from −0.60 to −0.29 (mean: −0.43) and wet season AW ranges from 0.80 to 1.22 (mean: 1.07). Eighteen of 20 models agree on the sign of change for a decrease in dry season AW (RCP8.5). All 20 models indicate a global increase in wet season AW (RCP8.5). The multimodel mean global land average dry season AW decreases from -0.38 ± 0.03 to -0.43 ± 0.03 (13% decrease, RCP8.5) and wet season AW increases from 0.94 ± 0.04 to 1.07 ± 0.06 (14% increase, RCP8.5).

We repeated the analysis using RCP4.5 and RCP2.6 projections. For RCP2.6, only 16 models were available at the time of the study (Figure 4). A general tendency of decreasing AW in dry season and increasing AW in wet season, compared to historical climate, is also found in RCP4.5 and RCP2.6 projections (Figure 2 and Table 1). Compared to the RCP8.5 scenario, the magnitudes are 47% less in the RCP4.5 scenario (range: 33%–75%) and 64% less in the RCP2.6 scenario (range: 40%–81%, Table 1). Particularly in the RCP2.6 scenario, AW changes are mostly within the uncertainty bounds of AW in the present climate (Figures 2

Table 1. A Comparison of AW Projections in RCP8.5, RCP4.5, and RCP2.6 Scenarios Relative to Historical Climate[a]

	Historical (1961–1990)	RCP8.5 (2070–2099)	RCP4.5 (2070–2099)	RCP2.6 (2070–2099)	% Benefits relative to RCP8.5 RCP 4.5	RCP 2.6
Dry season						
North America (JJA)	-0.22 ± 0.07	-0.36 ± 0.08	-0.31 ± 0.08	-0.25 ± 0.09	36	79
Russia (MJJ)	-0.21 ± 0.04	-0.36 ± 0.05	-0.30 ± 0.05	-0.27 ± 0.05	40	60
India (JFM)	-0.29 ± 0.06	-0.37 ± 0.07	-0.33 ± 0.07	-0.33 ± 0.07	50	50
Global (Local)	-0.38 ± 0.03	-0.43 ± 0.03	-0.41 ± 0.03	-0.41 ± 0.03	40	40
Wet season						
North America (NDJ)	0.57 ± 0.04	0.66 ± 0.05	0.63 ± 0.05	0.60 ± 0.05	33	67
Russia (OND)	0.80 ± 0.04	1.03 ± 0.04	0.93 ± 0.04	0.89 ± 0.04	43	61
India (JAS)	1.15 ± 0.24	1.59 ± 0.31	1.39 ± 0.27	1.29 ± 0.32	45	68
Global (Local)	0.94 ± 0.04	1.07 ± 0.06	1.01 ± 0.05	0.99 ± 0.05	46	62
Cumulative frequency (CF) less than a given threshold in local dry season						
North America ($CF \leq -1.0$)	2.7 ± 1.3	5.7 ± 2.4	4.4 ± 2.4	3.5 ± 2.2	43	73
Russia ($CF \leq -1.0$)	4.7 ± 1.7	12.3 ± 2.8	8.3 ± 2.5	7.5 ± 2.7	53	63
India ($CF \leq -1.5$)	3.0 ± 1.7	6.2 ± 2.8	3.8 ± 1.9	4.4 ± 2.5	75	56
CF greater than a given threshold in local wet season						
North America ($CF \geq 1.5$)	3.7 ± 0.9	7.4 ± 1.5	5.6 ± 1.3	4.4 ± 1.4	49	81
Russia ($CF \geq 1.5$)	3.1 ± 0.9	20.9 ± 3.9	10.8 ± 2.0	7.4 ± 1.9	57	76
India ($CF \geq 3.0$)	4.0 ± 1.0	14.2 ± 4.8	8.7 ± 2.6	7.4 ± 3.1	54	67

[a]Percentage benefits in RCP4.5 and RCP2.6 scenarios relative to RCP8.5 are also shown. Multimodel mean and 2 standard error estimates from 20 CMIP5 climate models are given (16 models for RCP2.6). Only the multimodel mean is considered for percentage benefit calculation. Regions of North America, Russia, and India are delineated in Figure 3a.

and 4). Complete analysis results for RCP4.5 and RCP2.6 are presented in Figures S2–S7 in the supporting information.

4. Conclusion and Discussion

This study proposes a new metric that accounts for changes in both precipitation and actual evapotranspiration in a changing climate, and allows us to investigate seasonal changes in AW in the 21st century. The multimodel consensus suggests less reliable AW in the 21st century compared with the 20th century with both decreased water availability in the local dry season and increased water availability in the local wet season. The sign of the changes are robust across the 20 CMIP5 climate model simulations examined (RCP8.5). It is worth noting that we have considered only the biophysical constraints on water availability (changes in P and ET). Additional factors such as increased water demand to meet agricultural, industrial, and domestic water needs due to increasing population can further induce stress on water resources [*Gosling and Arnell*, 2013]. Also, we have used global climate model output to assess reliability. Use of global hydrological models with inputs from global climate models may have some impacts on the results [*Haddeland et al*., 2011], but it is unlikely to change the main conclusion of this study because generally biases get canceled out when we compare two climates within same set of models [*Kumar et al*., 2010].

The increase in wet season AW is mainly driven by the precipitation changes in the corresponding season (Figure S8 in the supporting information). However, for the dry season AW, the corresponding season precipitation change does not fully explain the AW changes for most of the world (Figure S8). In the local dry season, precipitation generally increases in several regions including India, midlatitude to high-latitude regions in the Northern Hemisphere except the Mediterranean and southwestern United States, and Mexico. However, corresponding season increases in ET are higher than those in precipitation (not shown). In the RCP8.5 scenario, the global land average increase in precipitation and ET are 6% and 13%, respectively, in the local dry season (% change calculated locally and then averaged). *Chou and Lan* [2012] found that

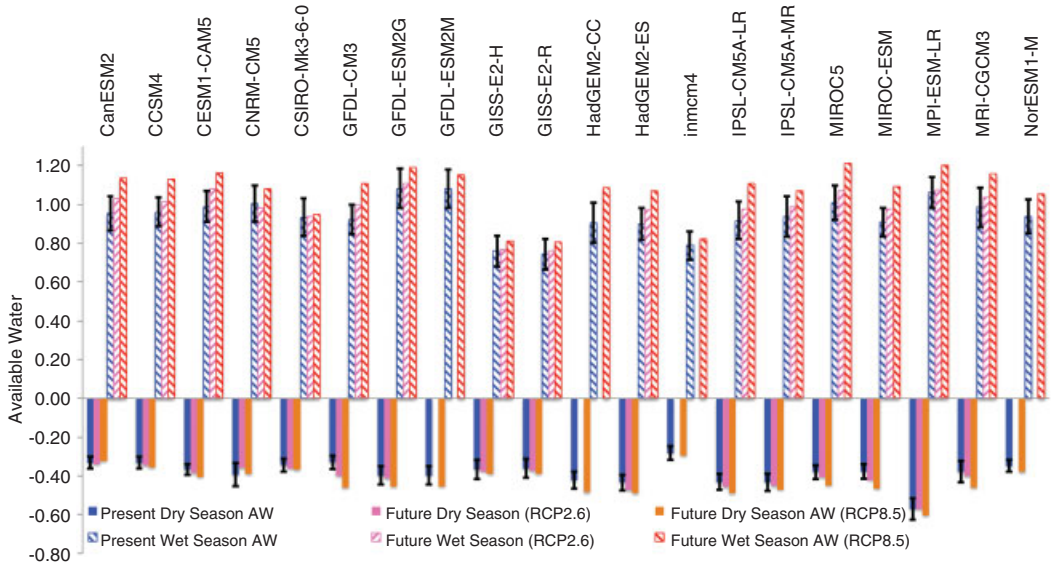

Figure 4. Intermodel spread in global land average (60°S–70°N) AW in historical (1961–1990) and RCP8.5 and RCP2.6 scenarios (2070–2099) in local dry and wet seasons. Error bar represents 2 climatological standard deviations. The 21st century changes greater than 2 climatological standard deviations (an indicator of natural climate variability) are significant at 95% confidence interval in this study.

under global warming scenarios, the increased annual precipitation range is driven by a larger upward trend in wet season precipitation with a smaller trend in dry season precipitation. *Dirmeyer et al*. [2013] found strong model consensus for soil moisture drying and expansion in the areas of soil moisture control (rather than available energy control) on evapotranspiration. It is likely that a number of counterbalancing factors such as increased evaporative demand from the atmosphere, drier land surface conditions, changes in snow cover at high latitudes and altitudes, and evolving land-atmosphere interactions are affecting the dry season AW.

Droughts are slowly evolving and relatively long term, i.e., phenomena lasting several months to years. Researchers and practitioners have employed several drought indices depending upon the application of drought identification, i.e., meteorological, hydrological, or agricultural [*Mishra and Singh*, 2010; *Sheffield et al*., 2012]. In this study, we focused on relatively short-term water deficits and their correlations with SPI. Correlations between AW and PDSI are lower than those between AW and SPI (not shown). We suggest that this is because of the autocorrelation characteristics of PDSI, whereas AW does not consider autocorrelation with the previous month. Further investigation is needed to consider specific drought characteristics such as duration, frequency, and intensity as well as their relationship with changes in AW.

Many previous studies have shown an increase in future total water availability in several midlatitude to high-latitude regions and India [*Milly et al*., 2005; *Arnell and Gosling*, 2013]. This study brings out an additional insight that even though annual mean water availability is increasing, seasonal climate changes can lead to significant reductions in dry season water availability.

There is general model consensus that future trends in water availability will align such that wet regions become wetter and dry regions become drier. This makes sense on theoretical grounds from thermodynamic (warmer climate leading to more atmospheric moisture) and dynamic arguments (warmer climate leading to greater uplift in ascending regions [*Biasutti*, 2013, and references therein]. Here we show that there is an analogous relationship on seasonal time scales. Generally, climate models suggest that the dry season becomes drier and the wet season becomes wetter, leading to an increasing likelihood of droughts and floods in seasons where drought and flood vulnerability is already high.

Acknowledgments

This study received support from the following grants: NSF 0947837, NSF 0830068, NOAA NA09OAR4310058, NOAA NA11OAR4310097, NASA NNX09AN50G, and U.S. Department of Energy, Cooperative Agreement DE-FC02-97ER62402. We acknowledge the World Climate Research Programme's Working Group on Coupled Modelling, which is responsible for CMIP, and we thank the climate modeling groups (shown in Figure 4) for producing and making available their model output. For CMIP the U.S. Department of Energy's Program for Climate Model Diagnosis and Intercomparison provides coordinating support and leads to the development of software infrastructure in partnership with the Global Organization for Earth System Science Portals. GLDAS2 data were acquired as part of the activities of NASA's Science Mission Directorate, and are archived and distributed by the Goddard Earth Sciences (GES) Data and Information Services Center (DISC). We also thank Jennifer Adams (Center for Ocean-Land-Atmosphere Studies) for acquiring CMIP5 data in time.

References

Arnell, N. W., and S. N. Gosling (2013), The impacts of climate change on river flow regimes at the global scale, *J. Hydrol.*, *486*, 351–364.

Biasutti, M. (2013), Future rise in rain inequality, *Nat. Geosci.*, *6*, 333–338.
Cao, L., G. Bala, K. Caldeira, R. Nemani, and G. Ban-Weiss (2010), Importance of carbon dioxide physiological forcing to future climate change, *PNAS, 107*, *21*, 9513–9518.
Chou, C., and C.-W. Lan (2012), Changes in the annual range of precipitation under global warming, *J. Clim.*, *25*, 222–235, doi:10.1175/JCLI-D-11-00097.1.
Chou, C., J. D. Neelin, C.-A. Chen, and J.-Y. Tu (2009), Evaluating the "Rich-Get-Richer" mechanism in tropical precipitation under global warming, *J. Clim.*, *22*, 1982–2005, doi:10.1175/2008JCLI2471.1.
Chou, C., J. C. H. Chiang, C.-W. Lan, C.-H. Chung, Y.-C. Liao, and C.-J. Lee (2013), Increase in the range between wet and dry season precipitation, *Nat. Geosci.*, *6*, 263–267, doi:10.1038/NGEO1744.
Dirmeyer, P. A., Y. Jin, B. Singh, and X. Yan (2013), Trends in land-atmosphere interactions from CMIP5 simulations, *J. Hydrometeorol.*, *14*, 829–849, doi:10.1175/JHM-D-12-0107.1.
Du, J., J. Feng, W. Xu, and P. Shi (2013), Analysis of dry/wet conditions using the standardized precipitation index and its potential usefulness for drought/flood monitoring in Hunan Province, China, *Stoch. Environ. Res. Risk Assess.*, *27*(2), 377–387.
Gosling, S. N., and N. W. Arnell (2013), A global assessment of the impact of climate change on water scarcity, *Clim. Change*, doi:10.1007/s10584-013-0853-x.
Haddeland, I., et al. (2011), Multimodel estimate of global terrestrial water balance: Setup and first results, *J. Hydrometeorol.*, *12*, 869–884.
Held, I. M., and B. J. Soden (2006), Robust responses of the hydrological cycle to global warming, *J. Clim.*, *19*, 5686–5699.
Keenan, T. F., D. Y. Hollinger, G. Bohrer, D. Dragoni, W. Munger, H. P. Schmid, and A. D. Richardson (2013), Increase in forest water-use efficiency as atmospheric carbon dioxide concentration rise, *Nature*, *499*, 324–327.
Kumar, S., and V. Merwade (2011), Evaluation of NARR and CLM3.5 outputs for surface water and energy budgets in the Mississippi River Basin, *J. Geophys. Res. Atmos.*, *116*, D08115, doi:10.1029/2010JD014909.
Kumar, S., V. Merwade, J. Kam, and K. Thurner (2009), Streamflow trends in Indiana: Effects of long term persistence, precipitation and subsurface drains, *J. Hydrol.*, *374*(1–2), 171–183.
Kumar, S., V. Merwade, W. Lee, L. Zhao, and C. Song (2010), Hydroclimatological impact of century-long drainage in midwestern United States: CCSM sensitivity experiments, *J. Geophys. Res. Atmos.*, *115*, D14105, doi:10.1029/2009JD013228.
Kumar, S., P. A. Dirmeyer, V. Merwade, T. DelSole, J. M. Adams, and D. Niyogi (2013), Land use/cover change impacts in CMIP5 climate simulations: A new methodology and 21st century challenges, *J. Geophys. Res. Atmos.*, *118*, 6337–6353, doi:10.1002/jgrd.50463.
McKee T. B., N. J. Doesken, and J. Kleist (1993), The relationship of drought frequency and duration to time scales, Preprints, *8th Conference on Applied Climatology*, pp. 179–184, Anaheim, Calif., 17–22 Jan.
Milly, P. C. D., K. A. Dunne, and A. V. Vecchia (2005), Global pattern of trends in streamflow and water available in a changing climate, *Nature*, *438*, 347–350, doi:10.1038/nature04312.
Mishra, A. K., and V. P. Singh (2010), A review of drought concepts, *J. Hydrol.*, *391*, 202–216.
Moss, R. H., et al. (2010), The next generation of scenarios for climate change research and assessment, *Nature*, *463*, 747–756.
Nature Editorial (2012), A first step, *Nature*, *486*, 439–440.
Okazaki, A., P. J.-F. Yeh, K. Yoshimura, M. Watanabe, M. Kimoto, and T. Oki (2012), Changes in flood risk under global warming estimated using MIROC5 and the discharge probability index, *J. Meteorol. Soc. Jpn.*, *90*(4), 509–524, doi:10.2151/jmsj.2012-405.
Palmer, W. C. (1965), Meteorological drought, *Res. Pap. 45*, U.S. Weather Bureau, Washington, D. C.
Riahi, K., S. Rao, V. Krey, C. Cho, V. Chirkov, G. Fisher, G. Kidermann, N. Nakicnovic, and P. Rafaj (2011), RCP8.5—A scenario of comparatively high greenhouse gas emissions, *Clim. Change*, *109*, 33–57.
Rind, D., R. Goldberg, J. Hansen, C. Rosenzweig, and R. Ruedy (1990), Potential evapotranspiration and the likelihood of future droughts, *J. Geophys. Res.*, *95*(D7), 9983–10003.
Rodell, M., et al. (2004), The global land data assimilation system, *Am. Meteorol. Soc.*, *85*, 381–394, doi:10.1175/BAMS-85-3-381.
Schuol, J., K. C. Abbaspour, H. Yang, R. Srinivasan, and A. J. B. Zehnder (2008), Modeling blue and green water availability in Africa, *Water Resour. Res.*, *44*, W07406, doi:10.1029/2007WR006609.
Seller, R. A., M. Hayes, and L. Bressan (2002), Using the standardized precipitation index for flood risk monitoring, *Int. J. Climatol.*, *22*, 1365–1376.
Sheffield, J., and E. F. Wood (2007), Characteristics of global and regional drought, 1950–2000: Analysis of soil moisture data from off-line simulation of the terrestrial hydrologic cycle, *J. Geophys. Res.*, *112*, D17115, 1–21, doi:10.1029/2006JD008288.
Sheffield, J., E. F. Wood, and M. L. Roderick (2012), Little change in global drought over the past 60 years, *Nature*, *491*, 435–438, doi:10.1038/nature11575.
Stricevic, R., N. Djurovic, and Z. Djurovic (2011), Drought classification in Northern Serbia based on SPI and statistical pattern recognition, *Meteorol. Appl.*, *18*(1), 60–69, doi:10.1002/met.207.
Tang, Q., and D. P. Lettenmaier (2012), 21st Century runoff sensitivities of major global river basins, *Geophys. Res. Lett.*, *39*, L06403, doi:10.1029/ 2011GL050834.
Taylor, K. E., R. J. Stouffer, and G. A. Meehl (2012), An overview of CMIP5 and the experiment design, *Bull. Am. Meteorol. Soc.*, *93*, 485–498, doi:10.1175/BAMS-D-11-00094.1.
Tollefson, J., and N. Gilbert (2012), Rio report card, *Nature*, *486*, 20–23.
UCAR/NCAR/CISL/VETS (2013), *The NCAR Command Language (NCL, Version 6.1.2) [Software]*, UCAR/NCAR/CISL/VETS, Boulder, Colo. [Available at http://dx.doi.org/10.5065/D6WD3XH5.]
van Vuuren, D. P., et al. (2011), The representative concentration pathways: An overview, *Clim. Change*, *109*, 5–31.